

OKHEP-99-05

Solution of Schwinger-Dyson Equations for \mathcal{PT} -Symmetric Quantum Field Theory

Carl M. Bender,^{1,*} Kimball A. Milton,^{2†} and Van M. Savage^{1‡}

¹*Department of Physics, Washington University, St. Louis, Missouri 63130, USA*

²*Department of Physics and Astronomy, University of Oklahoma, Norman, Oklahoma 73019, USA*

(July 14, 2018)

Abstract

In recent papers it has been observed that non-Hermitian Hamiltonians, such as those describing $ig\phi^3$ and $-g\phi^4$ field theories, still possess real positive spectra so long as the weaker condition of \mathcal{PT} symmetry holds. This allows for the possibility of new kinds of quantum field theories that have strange and quite unexpected properties. In this paper a technique based on truncating the Schwinger-Dyson equations is presented for renormalizing and solving such field theories. Using this technique it is argued that a $-g\phi^4$ scalar quantum field theory in four-dimensional space-time is renormalizable, is asymptotically free, has a nonzero value of $\langle 0|\phi|0 \rangle$, and has a positive definite spectrum. Such a theory might be useful in describing the Higgs boson.

11.15.Pg, 11.30.Qc, 25.75.-q, 3.65.-w

Typeset using REVTEX

*electronic mail: cmb@howdy.wustl.edu

†electronic mail: milton@mail.nhn.ou.edu

‡electronic mail: vmsavage@hbar.wustl.edu

]

I. INTRODUCTION

It has recently been observed [1,2] that quantum mechanical theories whose Hamiltonians are \mathcal{PT} -symmetric have positive definite spectra even if the Hamiltonian is not Hermitian. A class of such theories that has been studied extensively is defined by the Hamiltonian

$$H = p^2 - (ix)^N \quad (N \geq 2). \quad (1.1)$$

It is believed that the reality and positivity of the spectra are a direct consequence of \mathcal{PT} symmetry.

The positivity of the spectra for all N is an extremely surprising result; it is not at all obvious, for example, that the Hamiltonian $H = p^2 - x^4$ corresponding to $N = 4$ has a positive real spectrum. To understand this result it is necessary to define properly the boundary conditions in the corresponding Schrödinger equation.

For the Hamiltonian in Eq. (1.1) the Schrödinger differential equation corresponding to the eigenvalue problem $H\psi = E\psi$ is

$$-\psi''(x) - (ix)^N \psi(x) = E\psi(x). \quad (1.2)$$

The boundary conditions for this equation are discussed in detail in Ref. [1]. There, it was shown how to continue analytically in the parameter N away from the harmonic oscillator value $N = 2$. This analytic continuation defines the boundary conditions in the complex- x plane. The regions in the cut complex- x plane in which $\psi(x)$ vanishes exponentially as $|x| \rightarrow \infty$ are *wedges*. In Ref. [1] the wedges for $N > 2$ were chosen to be analytic continuations of the wedges for the harmonic oscillator, which are centered about the negative and positive real axes and have angular opening $\frac{\pi}{2}$. For arbitrary $N > 2$ the anti-Stokes' lines at the centers of the left and right wedges lie below the real axis at the angles

$$\begin{aligned} \theta_{\text{left}} &= -\pi + \left(\frac{N-2}{N+2}\right) \frac{\pi}{2}, \\ \theta_{\text{right}} &= -\left(\frac{N-2}{N+2}\right) \frac{\pi}{2}. \end{aligned} \quad (1.3)$$

The opening angle of these wedges is $\frac{2\pi}{N+2}$. In Ref. [1] the time-independent Schrödinger equation was integrated numerically inside the wedges to determine the eigenvalues to high precision.

The quantum mechanical Hamiltonian in Eq. (1.1) has additional remarkable properties. For example, for all $N > 2$ the expectation value $\langle 0|x|0 \rangle$ of the position operator x in the ground state is nonzero. This surprising result is true even when $N = 4$ [1].

These results for quantum mechanics raise some interesting questions regarding quantum field theory. In particular, does the self-interacting scalar quantum field theory defined by the Lagrangian

$$\mathcal{L} = \frac{1}{2}(\partial\phi)^2 + \frac{1}{2}m^2\phi^2 - \frac{g}{N}(i\phi)^N \quad (1.4)$$

have a positive definite spectrum and a nonvanishing value of $\langle 0|\phi|0 \rangle$ for all $N > 2$? We believe that the answer to this question is yes. Because of these properties, we believe that when $N = 4$ the resulting quantum field theory in four-dimensional space-time could serve as a good description of the Higgs particle. As we argue in this paper, the $-g\phi^4$ theory is particularly advantageous because, like the conventional $g\phi^4$ it has a dimensionless coupling constant, but unlike the conventional theory, it is asymptotically free and is thus not a trivial theory.

The question of how to determine the properties of \mathcal{PT} -symmetric non-Hermitian quantum field theories has already been examined. As we will see in this paper, conventional Feynman diagrammatic perturbation theory is not adequate for studying these theories. Thus, in previous work [3,4] the perturbative approach that was used was to take $N = 2 + \delta$, where δ is treated as a small parameter. While some interesting results regarding parity violation [3] and supersymmetry [4] were obtained, unfortunately this perturbative scheme has a severe drawback: It is not known how to carry out the renormalization procedure required to understand higher-dimensional theories.

Why is it that Feynman diagrams cannot be used to perform calculations in theories such as $-g\phi^4$? As we have already stated, in this theory $\langle 0|\phi|0 \rangle \neq 0$. There is no way to obtain this result using the standard Feynman rules; one cannot obtain a one-point Green's function using four-point vertex amplitudes. Indeed, as we will show in Sec. III in the context of zero-dimensional theories, the standard Feynman rules are incorrect for this theory.

In this paper we perform a systematic truncation of the Schwinger-Dyson equations as a calculational procedure. This idea has already been applied in a simple context to obtain Green's functions and energy levels in conventional quantum mechanical problems [5]. Truncating the Schwinger-Dyson equations is an inherently variational approach; including more and more of the higher Green's functions is equivalent to enlarging the space of variational parameters. In a recent study of the \mathcal{PT} -symmetric, non-Hermitian quantum mechanical Hamiltonian in Eq. (1.1) variational methods were found to be extremely accurate [6].

This paper is organized as follows: In Sec. II we review the general approach used in this paper. We show how to derive the Schwinger-Dyson equations using simple functional methods and we explain our truncation procedure. In Sec. III we examine the numerical accuracy of our truncation method in the context of zero-dimensional field theory. We study the massless zero-dimensional version of Eq. (1.4) in very high order in the truncation process for the cases $N = 3$ and $N = 4$. In the case of a zero-dimensional massive theory we show that the Feynman rules are inapplicable. In Sec. IV we examine the theory in Eq. (1.4) in one-dimensional space-time (quantum mechanics). Finally, in Sec. V we apply our methods to field theory in arbitrary dimension. As an application of our procedure we calculate the Callan-Symanzik function $\beta(g)$ for a four-dimensional $-g\phi^4$ theory for small g . We show that to leading order $\beta(g)$ is negative and thus the theory is asymptotically free. This result is in distinct contrast with the result for a conventional $g\phi^4$ theory.

II. ELEMENTARY DERIVATION OF THE SCHWINGER-DYSON EQUATIONS

The Schwinger-Dyson equations are an infinite set of coupled equations relating the Green's functions of a quantum field theory. In this section we derive the Schwinger-Dyson

equations using elementary formal functional methods.

We begin with Eq. (1.4) and append a term that represents the coupling of the field $\phi(x)$ to an external c -number source $J(x)$:

$$\mathcal{L} = \frac{1}{2}(\partial\phi)^2 + \frac{1}{2}m^2\phi^2 - \frac{g}{N}(i\phi)^N - J\phi. \quad (2.1)$$

This Lagrangian represents a self-interacting scalar quantum field theory in D -dimensional Euclidean space-time. If we vary the action with respect to $\phi(x)$ we obtain the field equation:

$$-\partial^2\phi(x) + m^2\phi(x) - ig[i\phi(x)]^{N-1} = J(x). \quad (2.2)$$

Next, leaving the source turned on, we take the expectation value of the field equation (2.2) in the vacuum state of the theory $|0\rangle$ and divide by the vacuum-vacuum functional $Z[J] = \langle 0|0\rangle$:

$$-\partial^2G_1^{(J)}(x) + m^2G_1^{(J)}(x) - gi^N\frac{\langle 0|\phi^{N-1}(x)|0\rangle}{\langle 0|0\rangle} = J(x), \quad (2.3)$$

where $G_1^{(J)}(x)$ is the one-point Green's function in the presence of the external source:

$$G_1^{(J)}(x) \equiv \frac{\langle 0|\phi(x)|0\rangle}{\langle 0|0\rangle}. \quad (2.4)$$

Note that the function $J(x)$ appears alone on the right side of Eq. (2.3) because it is a c -number and therefore can be factored out of matrix elements.

The objective is now to use Eq. (2.3) to calculate the Green's functions of the theory. The (connected) Green's functions in the presence of the source J are defined as functional derivatives of the logarithm of $Z[J]$ with respect to the source $J(x)$:

$$G_n^{(J)}(x_1, x_2, \dots, x_n) \equiv \frac{\delta^n}{\delta J(x_1)\delta J(x_2)\dots\delta J(x_n)} \ln(Z[J]). \quad (2.5)$$

To obtain the standard connected Green's functions of the theory (the connected part of the vacuum expectation value of the time-ordered product of the fields; that is, the sum of the connected n -point Feynman diagrams) we then turn off the source:

$$G_n(x_1, x_2, \dots, x_n) = G_n^{(J)}(x_1, x_2, \dots, x_n) \Big|_{J \equiv 0}. \quad (2.6)$$

Note that turning off the source restores translation invariance. As a result, the one-point Green's function G_1 is a constant independent of x , the two-point Green's function depends only on the difference $x - y$, $G_2(x, y) = G_2(x - y)$, $G_3(x, y, z) = G_3(x - y, x - z)$ depends on two differences, and so on.

Before one can proceed, one must express the third term in Eq. (2.3) in terms of the connected Green's functions of the theory. To do this we recall that functionally differentiating with respect to $J(x)$ is equivalent to inserting $\phi(x)$ in matrix elements [5].

Let us consider the simple case $N = 3$. In this case it is necessary to calculate the quantity $\langle 0|\phi^2(x)|0\rangle$. To do so we begin with Eq. (2.4) multiplied by $Z[J]$:

$$G_1^{(J)}(x)Z[J] = \langle 0|\phi(x)|0\rangle. \quad (2.7)$$

Taking the functional derivative of this equation with respect to $J(x)$ gives

$$[G_1^{(J)}(x)]^2 Z[J] + G_2^{(J)}(x, x) Z[J] = \langle 0|\phi^2(x)|0\rangle. \quad (2.8)$$

Hence, we can eliminate $\langle 0|\phi^2(x)|0\rangle$ from Eq. (2.3) to obtain

$$-\partial^2 G_1^{(J)}(x) + m^2 G_1^{(J)}(x) + gi \left([G_1^{(J)}(x)]^2 + G_2^{(J)}(x, x) \right) = J(x). \quad (2.9)$$

We now obtain the first of the Schwinger-Dyson equations by setting $J \equiv 0$ (turning off the source):

$$m^2 G_1 + gi \left[G_1^2 + G_2(0) \right] = 0. \quad (2.10)$$

Remember that by translation invariance G_1 is a constant, so that its derivative vanishes and that $G_2(0) = G_2(x - x) = G_2(x, x)$.

To obtain the second of the Schwinger-Dyson equations for $N = 3$ we take a functional derivative of Eq. (2.9) with respect to $J(y)$,

$$-\partial^2 G_2^{(J)}(x, y) + m^2 G_2^{(J)}(x, y) + gi \left[2G_1^{(J)}(x)G_2^{(J)}(x, y) + G_3^{(J)}(x, x, y) \right] = \delta(x - y), \quad (2.11)$$

and then set $J \equiv 0$ in this equation:

$$-\partial^2 G_2(x - y) + m^2 G_2(x - y) + gi [2G_1 G_2(x - y) + G_3(0, x - y)] = \delta(x - y). \quad (2.12)$$

If we continue the process of functionally differentiating with respect to J and setting $J \equiv 0$, we obtain the infinite tower of coupled differential equations known as the Schwinger-Dyson equations. For example, the third in the sequence is

$$\begin{aligned} & -\partial^2 G_3(x - y, x - z) + m^2 G_3(x - y, x - z) \\ & + gi [2G_1 G_3(x - y, x - z) + 2G_2(x - z)G_2(x - y) + G_4(0, x - y, x - z)] = 0. \end{aligned} \quad (2.13)$$

Note that these Schwinger-Dyson equations are *incomplete* in the sense that there are too many unknowns. The first equation contains G_1 and G_2 , the second contains G_1 , G_2 , and G_3 , and so on. Thus, each new equation contains a new unknown Green's function and the system never closes. However, we can force the system to close by truncating the sequence of coupled equations and setting $G_{n+1} = 0$ in the last equation. We will use this method throughout the remainder of the paper.

As a second example we derive the first four Schwinger-Dyson Equations from Eq. (2.3) for the case $N = 4$. Using the same approach as we did for the case $N = 3$, we begin by reexpressing $\langle 0|\phi^3(x)|0\rangle$. We do this by taking the functional derivative of Eq. (2.8) with respect to $J(x)$ to obtain

$$[G_1^{(J)}(x)]^3 Z[J] + 3G_1^{(J)}(x)G_2^{(J)}(x, x)Z[J] + G_3^{(J)}(x, x, x)Z[J] = \langle 0|\phi^3(x)|0\rangle. \quad (2.14)$$

Substituting this result into the $N = 4$ version of Eq. (2.3), we have

$$-\partial^2 G_1^{(J)}(x) + m^2 G_1^{(J)}(x) - g \left([G_1^{(J)}(x)]^3 + 3G_1^{(J)}(x)G_2^{(J)}(x, x) + G_3^{(J)}(x, x, x) \right) = J(x). \quad (2.15)$$

We obtain the first *Schwinger-Dyson* equation for $N = 4$ by setting $J \equiv 0$:

$$m^2 G_1 - g \left[G_1^3 + 3G_1 G_2(0) + G_3(0, 0) \right] = 0. \quad (2.16)$$

Using the same procedure as for $N = 3$ we now take a functional derivative of Eq. (2.15) with respect to $J(y)$ to obtain

$$\begin{aligned} & -\partial^2 G_2^{(J)}(x, y) + m^2 G_2^{(J)}(x, y) - g \left(3[G_1^{(J)}(x)]^2 G_2^{(J)}(x, y) \right. \\ & \left. + 3G_1^{(J)}(x)G_3^{(J)}(x, x, y) + 3G_2^{(J)}(x, x)G_2^{(J)}(x, y) + G_4^{(J)}(x, x, x, y) \right) = \delta(x - y). \end{aligned} \quad (2.17)$$

Now, setting $J \equiv 0$ gives the second of the *Schwinger-Dyson* equations for $N = 4$:

$$\begin{aligned} & -\partial^2 G_2(x - y) + m^2 G_2(x - y) - g[3G_1^2 G_2(x - y) \\ & + 3G_2(0)G_2(x - y) + 3G_1 G_3(0, x - y) + G_4(0, 0, x - y)] = \delta(x - y). \end{aligned} \quad (2.18)$$

Repeating this process once more by functionally differentiating Eq. (2.17) with respect to $J(z)$ and setting $J \equiv 0$ gives

$$\begin{aligned} & -\partial^2 G_3(x - y, x - z) + m^2 G_3(x - y, x - z) \\ & -g[6G_1 G_2(x - y)G_2(x - z) + 3G_1^2 G_3(x - y, x - z) \\ & + 3G_2(x - z)G_3(0, x - y) + 3G_2(x - y)G_3(0, x - z) + 3G_2(0)G_3(x - y, x - z) \\ & + 3G_1 G_4(0, x - y, x - z) + G_5(0, 0, x - y, x - z)] = 0, \end{aligned} \quad (2.19)$$

the third of the *Schwinger-Dyson* equations for $N = 4$. The fourth *Schwinger-Dyson* equation is

$$\begin{aligned} & -\partial^2 G_4(x - y, x - z, x - w) + m^2 G_4(x - y, x - z, x - w) \\ & -g[6G_2(x - y)G_2(x - z)G_2(x - w) + 6G_1 G_2(x - y)G_3(x - z, x - w) \\ & + 6G_1 G_2(x - z)G_3(x - y, x - w) + 6G_1 G_2(x - w)G_3(x - y, x - z) \\ & + 3G_3(0, x - y)G_3(x - z, x - w) + 3G_3(0, x - z)G_3(x - y, x - w) \\ & + 3G_3(0, x - w)G_3(x - y, x - z) + 3G_1^2 G_4(x - y, x - z, x - w) \\ & + 3G_2(x - y)G_4(0, x - z, x - w) + 3G_2(x - z)G_4(0, x - y, x - w) \\ & + 3G_2(x - w)G_4(0, x - y, x - z) + 3G_2(0)G_4(x - y, x - z, x - w) \\ & + 3G_1 G_5(0, x - y, x - z, x - w) + G_6(0, 0, x - y, x - z, x - w)] = 0. \end{aligned} \quad (2.20)$$

Again, we observe that the set of equations is incomplete; for this case the number of unknown Green's functions is two more than the number of equations (instead of one more as in the case $N = 3$). That is, the first equation for $N = 4$ contains the three unknowns G_1 , G_2 , and G_3 , the second contains G_1 , G_2 , G_3 , and G_4 , and so on. To solve this system of equations we truncate after the n th equation, but now to close the system of equations we must set $G_{n+1} = 0$ and $G_{n+2} = 0$ in the last and next to last equations.

How do we generalize this derivation to arbitrary N ? Clearly, when N is an *integer* and $N > 2$ we can use the two cases $N = 3$ and $N = 4$ discussed above as paradigms. All that

is needed is to functionally differentiate Eq. (2.7) $N - 2$ times. This gives an expression for $\langle 0|\phi^{N-1}(x)|0\rangle$ in Eq. (2.3). For example, when $N = 5$ we have

$$Z[J] \left([G_1^{(J)}(x)]^4 + 6[G_1^{(J)}(x)]^2 G_2^{(J)}(x, x) + 3[G_2^{(J)}(x, x)]^2 + 4G_1^{(J)}(x) G_3^{(J)}(x, x, x) + G_4^{(J)}(x, x, x, x) \right) = \langle 0|\phi^4(x)|0\rangle, \quad (2.21)$$

when $N = 6$, we have

$$Z[J] \left([G_1^{(J)}(x)]^5 + 10[G_1^{(J)}(x)]^3 G_2^{(J)}(x, x) + 15G_1^{(J)}(x) [G_2^{(J)}(x, x)]^2 + 10[G_1^{(J)}(x)]^2 G_3^{(J)}(x, x, x) + 10G_2^{(J)}(x, x) G_3^{(J)}(x, x, x) + 5G_1^{(J)}(x) G_4^{(J)}(x, x, x, x) + G_5^{(J)}(x, x, x, x, x) \right) = \langle 0|\phi^5(x)|0\rangle, \quad (2.22)$$

and so on. Once this calculation is completed, repeated functional differentiation with respect to J followed by setting $J \equiv 0$ gives the complete set of coupled Green's function equations.

Note that while these equations are rather complicated, they are easily expressible in terms of multinomial coefficients. Following the notation of Abramowitz and Stegun [7], the multinomial coefficients are defined as follows: For each integer n , there is a set of multinomial coefficients; each coefficient expresses the number of possible ways to partition $n = a_1 + 2a_2 + \dots + na_n$ different objects into a_k subsets containing k objects ($k = 1, 2, \dots, n$). For the first few integers n the sets of multinomial coefficients (called M_3 in Ref. [7]) are $\{1\}$ for $n = 1$, $\{1, 1\}$ for $n = 2$, $\{1, 3, 1\}$ for $n = 3$, $\{1, 4, 3, 6, 1\}$ for $n = 4$, and $\{1, 5, 10, 10, 15, 10, 1\}$ for $n = 5$. Observe that these are precisely the coefficients that appear in (2.7) for $\langle 0|\phi(x)|0\rangle$, (2.8) for $\langle 0|\phi^2(x)|0\rangle$, (2.14) for $\langle 0|\phi^3(x)|0\rangle$, (2.21) for $\langle 0|\phi^4(x)|0\rangle$, and (2.22) for $\langle 0|\phi^5(x)|0\rangle$. Also, in these equations the powers of the Green's functions are the numbers a_k .

To be precise, for each n we must take all possible combinations of the numbers a_k satisfying $n = a_1 + 2a_2 + \dots + na_n$. In the notation of Ref. [7], $\pi = 1^{a_1}, 2^{a_2}, \dots, n^{a_n}$. This allows us to read off the subscripts of the Green's functions and the powers to which they are raised; the numbers a_k are the powers and the numbers they exponentiate are the subscripts of the Green's functions in that term. From this we calculate the quantity

$$M_3 = (n; a_1, a_2, \dots, a_n) = \frac{n!}{(1!)^{a_1} a_1! (2!)^{a_2} a_2! \dots (n!)^{a_n} a_n!}, \quad (2.23)$$

which is the coefficient for that particular combination of Green's functions.

For example, given $\langle 0|\phi^3(x)|0\rangle$ there are three possible combinations of the numbers a_k that satisfy $n = a_1 + 2a_2 + \dots + na_n$: $a_1 = 3$; $a_1 = 1$ and $a_2 = 1$; and $a_3 = 1$. This gives $\pi = 1^3$; $\pi = 1, 2$; and $\pi = 3$. Thus, there are terms of the form G_1^3 , $G_1 G_2$, and G_3 . Calculating M_3 we find that the coefficients of these terms are 1, 3, and 1. Hence, we are able to reconstruct Eq. (2.14).

When N is noninteger, the situation is much more difficult. To derive an expression for $\langle 0|\phi^{N-1}(x)|0\rangle$ in this case, we assume first that N is integer and use the general formula for $\langle 0|\phi^{N-1}(x)|0\rangle$ in terms of multinomial coefficients. Then, in principle, we can continue analytically off the integers using analytical expressions in terms of Gamma functions for these multinomial coefficients.

Of course, this procedure is complicated, but we illustrate it below by considering the simplest truncation possible in which we keep only the first two Schwinger-Dyson equations and set $G_n = 0$ for all $n > 2$. In this case, for integer values of N we have the beautiful result that the only multinomial coefficients that appear are precisely the coefficients of the Hermite polynomials. Thus, for *noninteger* values of N we have parabolic cylinder functions with the exponential divided off. It is in this fashion that we are able to continue off the integers n .

To be explicit, we use the standard notation $D_\nu(x)$ to represent the parabolic cylinder function [8] and define the function $w_\nu(x)$ by

$$D_\nu(x) = e^{-x^2/4} x^\nu w_\nu(x). \quad (2.24)$$

Then, for integer N we factor $[G_1^{(J)}]^N$ out of the equation for $\langle 0 | \phi^N(x) | 0 \rangle$ and introduce the variables $\gamma^{(J)}$ and γ by

$$\gamma^{(J)} = \frac{iG_1^{(J)}(x)}{\sqrt{G_2^{(J)}(x, x)}} \quad \text{and} \quad \gamma = \frac{iG_1}{\sqrt{G_2(0)}}. \quad (2.25)$$

We then obtain for arbitrary noninteger N

$$\begin{aligned} \frac{\langle 0 | \phi^N(x) | 0 \rangle}{Z[J]} &= [G_1^{(J)}(x)]^N w_N(\gamma^{(J)}) \\ &= [G_1^{(J)}(x)]^N \sum_{k=0}^{\infty} \frac{(-1)^k N!}{(N-2k)! 2^k k! [\gamma^{(J)}]^{2k}}. \end{aligned} \quad (2.26)$$

(This series terminates if N is integer but is an infinite series if N is noninteger.) As we will see, when $J \equiv 0$, the constant G_1 is a negative imaginary number and the constant $G_2(0)$ is real and positive. Thus, the argument γ of w_N is real and positive.

Using Eq. (2.26) we write the field equation (2.3) explicitly in terms of the Green's functions of the theory:

$$-\partial^2 G_1^{(J)}(x) + m^2 G_1^{(J)}(x) - gi^N [G_1^{(J)}(x)]^{N-1} w_{N-1}(\gamma^{(J)}) = J(x). \quad (2.27)$$

(Remember that in the derivation of this equation we have discarded all Green's functions higher than G_2 .) As before, we obtain the first of the Green's functions for arbitrary N by setting the source $J \equiv 0$:

$$m^2 G_1 - gi^N G_1^{N-1} w_{N-1}(\gamma) = 0. \quad (2.28)$$

We obtain the second of the Schwinger-Dyson equations for arbitrary N by taking the functional derivative of Eq. (2.27) with respect to $J(y)$:

$$\begin{aligned} &-\partial^2 G_2^{(J)}(x, y) + m^2 G_2^{(J)}(x, y) \\ &- gi^N \left((N-1) [G_1^{(J)}(x)]^{N-2} G_2^{(J)}(x, y) w_{N-1}(\gamma^{(J)}) \right. \\ &\left. + i [G_1^{(J)}(x)]^{N-1} w'_{N-1}(\gamma^{(J)}) \frac{G_2^{(J)}(x, y)}{\sqrt{G_2^{(J)}(x, x)}} \right) = \delta(x - y), \end{aligned} \quad (2.29)$$

where we have set $G_3^{(J)} = 0$. Now, setting $J \equiv 0$ in the above equation yields the second of the Schwinger-Dyson equations:

$$-\partial^2 G_2(x - y) + m^2 G_2(x - y) - g i^N \left[(N - 1) G_1^{N-2} G_2(x - y) w_{N-1}(\gamma) + i G_1^{N-1} w'_{N-1}(\gamma) \frac{G_2(x - y)}{\sqrt{G_2(0)}} \right] = \delta(x - y). \quad (2.30)$$

This equation can be simplified by using the recurrence relations for parabolic cylinder functions [8],

$$x w'_{N-1}(x) = (N - 1)[w_{N-2}(x) - w_{N-1}(x)], \quad (2.31)$$

to obtain

$$-\partial^2 G_2(x - y) + m^2 G_2(x - y) + (N - 1)g(iG_1)^{N-2} w_{N-2}(\gamma) G_2(x - y) = \delta(x - y). \quad (2.32)$$

Thus, Eq. (2.28) and Eq. (2.32) are a closed system of two equations and two unknowns. The solution of this system for various choices of space-time dimension will be discussed in the following sections.

III. ZERO-DIMENSIONAL THEORIES

In zero-dimensional space-time the integral representation for the vacuum-vacuum functional $Z[J]$ corresponding to the Lagrangian in Eq. (1.4) is an ordinary integral

$$Z[J] = \int_{-\infty}^{\infty} d\phi \exp \left[-\frac{1}{2} m^2 \phi^2 + \frac{g}{N} (i\phi)^N + J\phi \right]. \quad (3.1)$$

To demonstrate the numerical accuracy of our truncation method we first study massless theories of the form in Eq. (3.1) where all quantities are exactly calculable. We find that for arbitrary N the Green's functions can be expressed exactly in terms of Gamma functions. Then, we examine massive theories and show that weak-coupling diagrammatic methods are inadequate for the analysis of \mathcal{PT} -symmetric theories.

A. Massless Theories in Zero Dimensions

Using Eqs. (3.1), (2.5), and (2.6) the expectation value of the field (the one-point connected Green's function) is

$$G_1 = -i \left(\frac{4N}{g} \right)^{1/N} \frac{\Gamma \left(\frac{1}{N} + \frac{1}{2} \right) \cos \left(\frac{\pi}{N} \right)}{\sqrt{\pi}}, \quad (3.2)$$

and the expectation value of the field squared is

$$\frac{\langle 0 | \phi^2 | 0 \rangle}{\langle 0 | 0 \rangle} = \left(\frac{N}{g} \right)^{2/N} \frac{\Gamma \left(\frac{3}{N} \right) \left[\sin^2 \left(\frac{\pi}{N} \right) - 3 \cos^2 \left(\frac{\pi}{N} \right) \right]}{\Gamma \left(\frac{1}{N} \right)}. \quad (3.3)$$

Using Eq. (2.8) with $J \equiv 0$ we express the two-point connected Green's function as $G_2 = \langle 0|\phi^2(x)|0\rangle/\langle 0|0\rangle - G_1^2$, which can be calculated exactly using the two equations given above.

Observe that for any $N \geq 2$, G_1 is pure imaginary and negative and G_2 is real and positive, as claimed earlier. This is in fact true in any dimension. The reality of G_2 and the imaginarity of G_1 follows from the \mathcal{PT} symmetry of these quantities. Applying \mathcal{P} to G_1 changes the sign, while applying \mathcal{P} to G_2 leaves the sign intact. Hence, under \mathcal{T} , which acts as complex conjugation, G_1 changes sign again and thus is pure imaginary, while G_2 does not change sign and thus is real.

The first truncation approximations to G_1 and G_2 obtained by keeping just the first two Schwinger-Dyson equations are found by solving the zero-dimensional massless versions of Eqs. (2.28) and (2.32). Observe that with $m = 0$, Eq. (2.28) demands that

$$w_{N-1}(\gamma) = 0. \quad (3.4)$$

In zero-dimensional space-time there are no derivatives with respect to x and the delta function is unity. Thus, all Schwinger-Dyson equations are algebraic. The second Schwinger-Dyson equation is

$$(N-1)g(iG_1)^{N-2}w_{N-2}(\gamma_0)G_2 = 1,$$

where γ_0 is the solution of Eq. (3.4). (Note that there is some ambiguity with regard to which zero to choose. Our numerical studies suggest that the most positive zero is always the correct choice, but we do not have a proof. We find that it is this zero that gives the most accurate numerical results.) Recalling the definition of γ , we insert $G_2 = -G_1^2/\gamma_0^2$ to obtain an expression for G_1 :

$$G_1 = -i \left[\frac{\gamma_0^2}{(N-1)gw_{N-2}(\gamma_0)} \right]^{1/N}. \quad (3.5)$$

Again using the definition of γ , we express G_2 as

$$G_2 = \left[\frac{\gamma_0^{2-N}}{(N-1)gw_{N-2}(\gamma_0)} \right]^{2/N}. \quad (3.6)$$

Table I compares the exact results with the corresponding first approximations for $N = 3$, $N = 4$, and $N = 5$.

Deriving an expression for the second approximation in terms of N is difficult. However, for a specific N , solving larger and larger systems of Schwinger-Dyson equations in which more and more Green's functions are included can be done symbolically on a computer. The case $N = 3$ is comparatively simple. If we keep n equations, then for $k < n$, the k th equation is linear in G_{k+1} . Thus, we can systematically solve a sequence of linear equations for the Green's functions, substitute the results into the n th equation, and solve the resulting polynomial equation for G_1 .

For $N = 3$, the first six approximations to $iG_1g^{1/3}$ are 0.79370, 0.69336, 0.74690, 0.71256, 0.73987, and 0.71237. The exact answer, taken from Eq. (3.2) with $N = 3$, is 0.72901 (see Table I). Note that the approximations oscillate around the correct answer. For the case of a Hermitian Hamiltonian we would expect that the approach to the correct answer is

monotone. This is because the calculation that we are performing is variational in nature. Keeping more and more Green's functions corresponds to enlarging the parameter space. However, in this case the Hamiltonian is not Hermitian, so this oscillation is not surprising. Indeed, it is consistent with our variational studies of \mathcal{PT} -symmetric quantum mechanical systems in Ref. [6].

Apart from the oscillations, we would hope that successive approximations would come closer to the correct value. Thus, the fact that the sixth approximation is worse than the fifth and that eventually most of the approximations become complex is a startling result. We believe that this is also due to the non-Hermiticity of the Hamiltonian. Indeed, while these approximations are numerically extremely accurate, we find that the convergence is rather slow and it may even be that this truncation method does not converge. To examine the convergence we have numerically solved *very large* systems of coupled Schwinger-Dyson equations for $N = 3$; we have plotted in Fig. 1 all solutions for the one-point Green's function in the complex plane for the system of 150 coupled Schwinger-Dyson equations that lie near the exact answer. In this figure we see that the algebraic solutions for the one-point Green's function form a very small *loop* around the exact value. The largest dimension of the loop is along the real axis and is approximately 0.04. The furthest distance of a point on the loop from the correct answer is approximately 0.034. A weighted average of the points on the loop is extremely close to the correct answer 0.72901.

The case $N = 4$ is more complicated than that of $N = 3$ because now the last two Schwinger-Dyson equations, rather than just the last equation, are nonlinear. As a result the largest number of equations we can solve and hence, the largest number of Green's functions we can include, is ten. The first five approximations to $iG_1g^{1/4}$ are 1.10668, 0.90560, 1.02988, 0.96159, and 1.02868. The exact value is 0.97774 (see Table I). Just as for $N = 3$, the approximations oscillate around the exact answer and successive approximations are numerically accurate but appear to converge very slowly. In this case, the fifth approximation is worse than the fourth. We have plotted in Fig. 2 all solutions of the first ten coupled Schwinger-Dyson equations for the one-point Green's function that lie near the exact answer. As in the case of Fig. 1 these solutions form a small loop in the complex plane around the exact answer.

The numerical work that we have done on zero-dimensional massless theories suggests that solving systems of truncated Schwinger-Dyson equations gives extremely accurate numerical approximations to the Green's functions. The convergence of the method is still not understood and warrants further study.

B. Massive Theories in Zero Dimensions

In zero-dimensional space-time, massless theories are so simple that it is possible to solve the Schwinger-Dyson equations as algebraic systems. However, in higher dimensions, the coupled Schwinger-Dyson equations are quite complicated. Thus, we will be interested in obtaining perturbative solutions for the case of small coupling constant g .

To gain a rudimentary understanding of the perturbative nature of the theories in Eq. (1.4), we study in this subsection the path-integral expressions for the n -point *disconnected* Green's functions F_n of a zero-dimensional $-g\phi^4$ field theory. These disconnected

Green's functions are expressed as ratios of integrals:

$$F_n = \frac{\int_{-\infty}^{\infty} d\phi \phi^n \exp\left(-\frac{1}{2}m^2\phi^2 + \frac{g}{4}\phi^4\right)}{\int_{-\infty}^{\infty} d\phi \exp\left(-\frac{1}{2}m^2\phi^2 + \frac{g}{4}\phi^4\right)}. \quad (3.7)$$

Although these integrals cannot be done exactly, we can use the method of steepest descents to obtain an asymptotic result for small g with m fixed. We will see that, depending on whether the sign of m^2 is positive or negative, we obtain drastically different results.

We begin by replacing ϕ by the dimensional quantity x according to $\phi = \sqrt{2/g|m|}x$. This gives

$$F_n = \left(\frac{2|m|^2}{g}\right)^{n/2} \frac{\int_{-\infty}^{\infty} dx x^n \exp[-\Lambda(\pm x^2 - x^4)]}{\int_{-\infty}^{\infty} dx \exp[-\Lambda(\pm x^2 - x^4)]}, \quad (3.8)$$

where $\Lambda = m^4/g$ is a large positive parameter as $g \rightarrow 0$ and we have distinguished between the two cases $m^2 > 0$ and $m^2 < 0$.

To calculate the integrals in Eq. (3.7) asymptotically, we find the stationary points of the function $\rho(x)$ in the exponent, where

$$\rho(x) = \pm x^2 - x^4. \quad (3.9)$$

Setting the derivative of this function equal to zero gives the solutions $x = 0, \pm 1/\sqrt{2}$ for $m^2 > 0$ and $x = 0, \pm i/\sqrt{2}$ for $m^2 < 0$. These stationary points are shown on Figs. 3 and 4.

Next, we find the paths of steepest ascent and descent that pass through these stationary points. Substituting $x = u + iv$ into Eq. (3.9) and separating the real and imaginary parts yields

$$\rho(u + iv) = \pm(u^2 - v^2) - u^4 - v^4 + 6u^2v^2 + i[\pm 2uv - 4uv(u^2 - v^2)]. \quad (3.10)$$

Thus, the paths along which $\text{Im } \rho = 0$ are given by $u = 0, v \neq 0$; $v = 0, u \neq 0$; and $u^2 = v^2 \pm 1/2$, where the \pm depends on the sign of m^2 .

To determine whether each of these paths is a steepest ascent or descent path, we perform a local analysis of the paths at each of the saddle points. The results of this analysis are displayed in Figs. 3 and 4. The stationary phase contour is chosen such that the boundary conditions are obeyed. Using Eq. (1.3), we choose the end points that lie below the real axis at the angles $-\pi/6$ and $-5\pi/6$. For $m^2 > 0$ the contour follows the path $u = -\sqrt{v^2 + 1/2}$ from the lower left quadrant of the complex- x plane up to the stationary point at $-1/\sqrt{2}$, then goes along the real axis from $-1/\sqrt{2}$ through the stationary points at the origin and at $1/\sqrt{2}$, and finally leaves the point $1/\sqrt{2}$ and follows the path $u = \sqrt{v^2 + 1/2}$ down to the lower right quadrant of the complex- x plane. For $m^2 < 0$ the contour follows the path $v = -\sqrt{u^2 + 1/2}$, which passes through the stationary point at $-i/\sqrt{2}$.

Now, we determine the disconnected Green's functions F_n for both the $m^2 > 0$ and $m^2 < 0$ cases by evaluating the integrals in Eq. (3.8) along the appropriate stationary phase contours. For $m^2 > 0$ the Green's functions with odd subscript vanish (by oddness) along the part of the contour that lies on the real axis. Evaluating the integrals asymptotically

along the remaining parts of the contour gives an exponentially small result; apart from a multiplicative constant

$$F_{2n+1} \sim g^{-n-1/2} e^{-\Lambda/4} \quad (g \rightarrow 0^+). \quad (3.11)$$

The dominant contribution to Green's functions of even subscript comes from the portion of the contour along the real axis. Evaluating the integrals near the saddle point at the origin, we find that the small- g behavior of these Green's functions is given by

$$F_{2n} \sim m^{-2n} \quad (g \rightarrow 0^+), \quad (3.12)$$

apart from a multiplicative constant. Note that the Green's functions with even subscript behave very differently than the Green's functions with odd subscript. Further, notice that the behavior of the Green's functions with odd subscript is inherently non-perturbative and, as a result, Feynman perturbative methods cannot be used to calculate these Green's functions.

For $m^2 < 0$ the dominant contribution to *all* of the Green's functions comes from the saddle point at $-i/\sqrt{2}$. As a result, *all* of the Green's functions exhibit similar behavior. To be specific, we have

$$F_n \sim (-i)^n |m|^n g^{-n/2} \quad (g \rightarrow 0^+). \quad (3.13)$$

Thus, once again, it is clear that these results cannot be obtained using Feynman diagrams. As we will see in Sec. V this theory is also the one that is asymptotically free in four dimensions and the more interesting of the two cases.

IV. NUMERICAL STUDY OF ONE-DIMENSIONAL THEORIES

Our success with zero-dimensional massless theories prompts us to study one-dimensional (quantum mechanical) massless theories of the form in Eq. (1.4). Numerical computations have been performed in one-dimension which allow us to compare with exact numbers [1].

In analogy with the last section, we find the first approximation to G_1 and G_2 by solving the one-dimensional massless versions of Eqs. (2.28) and (2.32). Observe that with $m = 0$ we obtain Eq. (3.4) once again. In fact, Eq. (3.4) holds independent of the dimension. The second Schwinger-Dyson equation is given by

$$-\partial^2 G_2(x - y) + (N - 1)g(iG_1)^{N-2} w_{N-2}(\gamma_0) G_2(x - y) = \delta(x - y). \quad (4.1)$$

This equation depends on the dimension D through the partial derivative. If we introduce the variable M defined by $M^2 = (N - 1)g(iG_1)^{N-2} w_{N-2}(\gamma_0)$, it is clear that Eq. (4.1) is just the equation for the Feynman propagator, whose solution in one-dimension can be written

$$G_2(x - y) = \frac{1}{2M} e^{-|x-y|}. \quad (4.2)$$

Consequently, $G_2(0) = 1/(2M)$. Recalling the definition of γ we use $G_2(0) = -G_1^2/\gamma_0^2$ as we did in the previous section to obtain an expression for G_1 :

$$G_1 = -i \left[\frac{\gamma_0^4}{4(N-1)gw_{N-2}(\gamma_0)} \right]^{1/(N+2)}. \quad (4.3)$$

Substituting G_1 into our expression for M yields

$$M = \left[(N-1)gw_{N-2}(\gamma_0) \left(\frac{\gamma_0}{\sqrt{2}} \right)^{N-2} \right]^{2/(N+2)}, \quad (4.4)$$

which further allows us to write $G_2(0)$ as

$$G_2(0) = \frac{1}{2} \left[\frac{1}{g(N-1)w_{N-2}(\gamma_0)} \left(\frac{\gamma_0}{\sqrt{2}} \right)^{2-N} \right]^{2/(N+2)}. \quad (4.5)$$

For field theories, M represents the renormalized mass, which is nothing more than the difference in energy between the first excited state and the ground state $E_1 - E_0$. Table II compares the exact values of M and G_1 with the corresponding first approximations for the cases $N = 3$, $N = 4$, and $N = 5$. (Here, we must set $g = N/2$ and multiply M by 2 to match the Lagrangians studied in Ref. [1].)

In one dimension it is difficult to obtain the second approximation, even for a specific N , because it requires solving coupled systems of nonlinear differential equations. As in the previous section, the easiest case to study is $N = 3$. The first three Schwinger-Dyson equations are given in Sec. I as Eqs. (2.10), (2.12), and (2.13) with $m = 0$. To close this system of equations we set $G_4 = 0$ and $z = y$. Then, the third Schwinger-Dyson equation becomes

$$-\partial^2 G_3(x-y) + gi[2G_1G_3(x-y) + 2G_2^2(x-y)] = 0. \quad (4.6)$$

Next, we Fourier transform the second and third Schwinger-Dyson equations to obtain

$$(p^2 + M^2)\tilde{G}_2(p) + gi\tilde{G}_3(p) = 1 \quad (4.7)$$

and

$$(p^2 + M^2)\tilde{G}_3(p) + 2gi \int_{-\infty}^{\infty} \frac{dq}{2\pi} \tilde{G}_2(q)\tilde{G}_2(p-q) = 0, \quad (4.8)$$

where we have used the same definition of M as above, the convolution property of Fourier transforms, and the translation invariance of Green's functions $G_3(0, x-y) = G_3(x-y, x-y) = G_3(x-y)$.

We now solve for $\tilde{G}_2(p)$ and obtain

$$\tilde{G}_2(p) = \frac{1}{p^2 + M^2} - \frac{2g^2}{(p^2 + M^2)^2} \int_{-\infty}^{\infty} \frac{dq}{2\pi} \tilde{G}_2(q)\tilde{G}_2(p-q). \quad (4.9)$$

The simplest approach to solving this nonstandard integral equation is to iterate it to high order in the small parameter g . This iterative procedure can be represented in terms of diagrams. These diagrams all have a similar structure: They begin with one line that

branches into two lines. This branching process continues until the maximum number of lines is attained. Then the process is reversed, with lines combining in pairs until only one line remains. We were able to perform the calculations symbolically on a computer. We calculated the propagator to order $O(g^{10})$; the first three terms in the expansion are

$$\begin{aligned}\tilde{G}_2(p) = & \frac{1}{p^2 + M^2} - \frac{2g^2}{M(p^2 + M^2)^2(p^2 + 4M^2)^2} \\ & + \frac{(456M^4 + 70M^2p^2 + 4p^4)g^4}{9M^6(p^2 + M^2)^2(p^2 + 4M^2)^2(p^2 + 9M^2)} + O(g^6).\end{aligned}\quad (4.10)$$

Now that we have $\tilde{G}_2(p)$ to high order in g , we make the *ansatz* that it can be expressed in the form

$$\tilde{G}_2(p) = \frac{Z_1}{p^2 + M_1^2} + \frac{Z_2}{p^2 + M_2^2} + \frac{Z_3}{p^2 + M_3^2} + \dots, \quad (4.11)$$

where $M_n = nM + b_{1,n}g^2 + b_{2,n}g^4 + b_{3,n}g^6 + \dots$, $Z_1 = 1 + a_{1,1}g^2 + a_{2,1}g^4 + a_{3,1}g^6 + \dots$, $Z_2 = a_{1,2}g^2 + a_{2,2}g^4 + a_{3,2}g^6 + \dots$, $Z_3 = a_{2,3}g^4 + a_{3,3}g^6 + \dots$, and so on. By matching this *ansatz* to our calculation, we determine the coefficients $a_{k,n}$ and $b_{k,n}$. [The expansion of the *ansatz* does not exactly match the expansion of our calculation. This is easily understood because our calculation for $\tilde{G}_2(p)$ only involves special diagrams described above, while the *ansatz* involves all types of diagrams. However, the system of equations is neither overdetermined nor underdetermined, so all coefficients may still be calculated.]

The series for the M_n are

$$\begin{aligned}M_1 &= M + \frac{g^2}{3M^4} - \frac{31g^4}{72M^9} + \frac{1279g^6}{1944M^{14}} - \frac{98287g^8}{93312M^{19}} + \frac{9641179g^{10}}{5598720M^{24}}, \\ M_2 &= 2M + \frac{2g^2}{3M^4} - \frac{11g^4}{108M^9} + \frac{133g^6}{1944M^{14}} + \frac{33161g^8}{279936M^{19}}, \\ M_3 &= 3M + \frac{g^2}{M^4} + \frac{29g^4}{216M^9} + \frac{101g^6}{486M^{14}}, \\ M_4 &= 4M + \frac{4g^2}{3M^4} + \frac{109g^4}{270M^9}, \\ M_5 &= 5M + \frac{5g^2}{3M^4}.\end{aligned}\quad (4.12)$$

Since we now have expressions for M_n in terms of M , we need only determine M accurately to finish the calculation. This is done using the first Schwinger-Dyson equation (2.10), which implies that

$$M^4 = 4g^2G_2(0). \quad (4.13)$$

Observe that

$$G_2(0) = \int_{-\infty}^{\infty} \frac{dp}{2\pi} \tilde{G}_2(p). \quad (4.14)$$

So, based on our calculation of the first three terms above, the first few terms are

$$G_2(0) = \frac{1}{2M} - \frac{g^2}{9M^6} + \frac{7g^4}{96M^{11}}. \quad (4.15)$$

This allows us to express M and g as

$$\begin{aligned} M^2 &= \sqrt{4g^2G_2(0)} \\ &= \sqrt{\frac{2g^2}{M} - \frac{4g^4}{9M^6} + \frac{7g^6}{24M^{11}} + \mathcal{O}(g^8)}. \end{aligned} \quad (4.16)$$

Keeping terms to order $\mathcal{O}(g^{10})$ we obtain $M = 1.126151g^{2/5}$.

With this value of M , the M_n become numerical series multiplied by an overall factor of $g^{2/5}$. Successive terms in this numerical series decrease in magnitude and thus the series appears to be convergent. To compare with the numerical results and match the Lagrangian in Ref. [1], we set $g = 3/2$ and multiply the M_n by 2; results are given in Table III.

V. SCHWINGER-DYSON EQUATIONS IN D DIMENSIONS

In this section we show how to solve truncated systems of Schwinger-Dyson equations in D dimensions. First, we consider the case $D < 2$, in which it is not necessary to perform any renormalization. Then we consider the case of arbitrary D , in which it is necessary to discuss renormalization.

A. Schwinger-Dyson Equations for $D < 2$

In this subsection we solve Eqs. (2.28) and (2.32) in arbitrary dimension D with $m = 0$. This calculation is a straightforward generalization of the one for $D = 1$.

As previously stated, when $m = 0$, Eq. (2.28) implies Eq. (3.4). In addition Eq. (2.32) continues to imply Eq. (4.1),

$$-\partial^2 G_2(x - y) + M^2 G_2(x - y) = \delta(x - y), \quad (5.1)$$

in which we have defined the renormalized mass M^2 by

$$M^2 = -g^N (N - 1) G_1^{N-2} w_{N-2}(\gamma_0). \quad (5.2)$$

Equation (5.1) is just the differential equation satisfied by the Feynman propagator.

We solve these two equations in arbitrary dimension D by taking the Fourier transform to obtain the propagator:

$$\tilde{G}_2(p) = 1/(p^2 + M^2). \quad (5.3)$$

Fourier transforming this propagator back to position space and then setting $x = y$ gives

$$G_2(0) = M^{D-2} \Gamma(1 - D/2) \pi^{-D/2} 2^{-D}. \quad (5.4)$$

Using Eqs. (2.25) and (5.2) we solve for G_1 :

$$G_1 = -i \left\{ [(N-1)gw_{N-2}(\gamma_0)]^{(D-2)/2} \Gamma(1-D/2)(4\pi)^{-D/2} \gamma_0^2 \right\}^{2/(-ND+2N+2D)}. \quad (5.5)$$

Substituting this result into Eq. (5.2) yields

$$M = \left\{ [(N-1)gw_{N-2}(\gamma_0)]^2 \left[\Gamma(1-D/2)(4\pi)^{-D/2} \gamma_0^2 \right]^{N-2} \right\}^{1/(-ND+2N+2D)}, \quad (5.6)$$

and substituting the last two results into Eq. (5.4) gives an expression for G_2 . These expressions reduce to the zero-dimensional and one-dimensional solutions given in the previous two sections. Notice that each of these expressions becomes singular at $D = 2$.

Using these approximate solutions we can determine the large- N behavior of the Greens functions as $N \rightarrow \infty$. To do so, we need to determine the asymptotic behavior of the zeros of the parabolic cylinder function. According to Ref. [9], the largest zero of $w_{n-1}(\gamma)$ for large n is given by $\gamma_0 \sim 2\sqrt{n}$. Substituting this into the integral representation for $w_{n-2}(\gamma)$ and using Eq. (2.31) we perform a steepest-descent calculation to obtain $w_{n-2} \sim \sqrt{2/\pi} 3^{-1/6} \Gamma(1/3) 2^{-n} n^{1/6} e^{n/2}$. We have verified these results numerically to high accuracy. Taking $N \rightarrow \infty$ in the expressions for G_1 , G_2 , and M above and using the asymptotic results for the parabolic cylinder function, we obtain

$$\begin{aligned} G_1 &\sim -2i/\sqrt{e} = -1.21306i, \\ G_2 &\sim 1/(Ne), \\ M^2 &\sim \left[e\Gamma(1-D/2)(4\pi)^{-D/2} N \right]^{2/(2-D)}. \end{aligned} \quad (5.7)$$

Observe that G_1 is independent of both N and D to this order, G_2 depends on N but not on D , and M^2 depends on both N and D . These results are valid for large N for all $D < 2$. These properties are evident in zero dimensions from Eqs. (3.2) and (3.3). While the behavior of G_1 and $\langle 0 | \phi^2(0) | 0 \rangle$ is correctly predicted, the behavior of G_2 is not because the first-order behaviors of G_1 and $\langle 0 | \phi^2(0) | 0 \rangle$ cancel, leaving a second-order term to describe G_2 . Also, this calculation predicts that M^2 increases like $N^{2/(2-D)}$. That is, for large N the separation between the energy levels diverges and hence, the energy levels must diverge. In $D = 1$ our approximation suggests that M grows like N . In fact, M grows like N^2 in $D = 1$ as discussed in Ref. [10]. This is the simplest possible truncation, but it suggests the correct behavior.

B. Perturbative Renormalization of the Schwinger-Dyson Equations in D -Dimensions and Leading-Order Calculation of the Beta Function

Let us first consider the \mathcal{PT} -symmetric $ig\phi^3$ theory in six space-time dimensions. The Green's functions for that theory are governed by the system of equations beginning with Eq. (2.10), (2.12), and (2.13). Let us seek a perturbative solution to this system of equations in which $G_n \sim g^{n-2}$. In leading order we have first, from Eq. (2.10),

$$G_1 = i \frac{m^2}{g}. \quad (5.8)$$

Then, from Eq. (2.12), the two-point function in momentum-space is

$$\tilde{G}_2(p) = \int d^6x e^{ip(x-y)} G_2(x-y) = \frac{1}{p^2 + M^2}, \quad (5.9)$$

where

$$M^2 = m^2 + 2igG_1 = -m^2. \quad (5.10)$$

Thus, in order to avoid unphysical singularities, we must have for this type of solution $m^2 < 0$. The leading solution to Eq. (2.13) is

$$\tilde{G}_3(p, q) = \frac{2ig}{(p^2 + M^2)(q^2 + M^2)[(p+q)^2 + M^2]}, \quad (5.11)$$

which has an obvious interpretation as a vertex with three external lines.

More generally, the solution to Eq. (2.10) is

$$G_1 = \frac{1}{2} \left[im^2/g \pm i\sqrt{(m^2/g)^2 + 4G_2(0)} \right], \quad (5.12)$$

which corresponds in the perturbative case, where $|G_2(0)| \ll (m^2/g)^2$, to

$$G_1 = \begin{cases} i\frac{m^2}{g}, \\ -i\frac{g}{m^2}G_2(0). \end{cases} \quad (5.13)$$

The second solution given in Eq. (5.13) corresponds to the usual perturbative tadpole contribution to the vacuum expectation value of the field, while the first is the new, nontrivial solution given in Eq. (5.8).

Perturbatively solving the next in the sequence of Schwinger-Dyson equations, we obtain for the four-point function in leading order

$$\begin{aligned} \tilde{G}_4(p, q, r) &= \frac{-2ig}{((p+q+r)^2 + M^2)(p^2 + M^2)(q^2 + M^2)(r^2 + M^2)} \\ &\times \left[\frac{1}{(p+q)^2 + M^2} + \frac{1}{(p+r)^2 + M^2} + \frac{1}{(q+r)^2 + M^2} \right]. \end{aligned} \quad (5.14)$$

Inserting this back into Eq. (2.13), we obtain the one-loop correction to the three-point function. Apart from a tadpole term, this is just the same as that found in the conventional ϕ^3 theory; correspondingly, the beta function is obtained from that in the conventional theory by the replacement $g \rightarrow ig$ (see, for example, Ref. [11])

$$\beta(g) = \mu \frac{\partial g}{\partial \mu} = \frac{3}{2} \left(\frac{g}{4\pi} \right)^3, \quad (5.15)$$

where $g(\mu)$ is the running coupling at scale μ . Unlike the usual ϕ_6^3 theory, the \mathcal{PT} symmetric theory given here is not asymptotically free.

Of course, the ϕ_4^4 theory is of far greater interest. In particular, it plays a crucial role in the standard model as the origin of particle masses through the Higgs mechanism. Yet the

triviality of that theory is a source of difficulty. What happens here, when we set $N = 4$ in Eq. (1.1)?

The first few Schwinger-Dyson equations are given in Eqs. (2.16), (2.18), (2.19), and (2.20). Note that the last three equations can be simplified through the introduction of the renormalized mass

$$M^2 = m^2 - 3gG_2(0) - 3gG_1^2. \quad (5.16)$$

Thus we obtain the following equations for the two-point function,

$$(-\partial^2 + M^2)G_2(x - y) - gG_1G_3(0, x - y) - gG_4(0, 0, x - y) = \delta(x - y), \quad (5.17)$$

the three-point function

$$\begin{aligned} & (-\partial^2 + M^2)G_3(x - y, x - z) - 6gG_1G_2(x - y)G_2(x - z) - 3g[G_2(x - y)G_3(0, x - z) \\ & + G_2(x - z)G_3(0, x - y)] - 3gG_1G_4(0, x - y, x - z) - gG_5(0, 0, x - y, x - z) = 0, \end{aligned} \quad (5.18)$$

and the four-point function

$$\begin{aligned} & (-\partial^2 + M^2)G_4(x - y, x - z, x - w) - 6gG_2(x - y)G_2(x - z)G_2(x - w) \\ & - 3g[G_2(x - y)G_4(0, x - z, x - w) + G_2(x - z)G_4(0, x - y, x - w) \\ & + G_2(x - w)G_4(0, x - y, x - z)] - 6gG_1[G_2(x - y)G_3(x - z, x - w) \\ & + G_2(x - z)G_3(x - y, x - w) + G_2(x - w)G_3(x - y, x - z)] \\ & - 3g[G_3(0, x - y)G_3(x - z, x - w) + G_3(0, x - z)G_3(x - y, x - w) \\ & + G_3(0, x - w)G_3(x - y, x - z)] - 3gG_1G_5(0, x - y, x - z, x - w) \\ & - 3gG_6(0, 0, x - y, x - z, x - w) = 0. \end{aligned} \quad (5.19)$$

Now there are two regimes. If $m^2 > 0$ the only consistent perturbative solution to the above system of equations is one in which the odd Green's functions are exponentially small, $G_{2n+1} \sim e^{-1/g}$, and the even and odd Green's functions decouple. [This result is analogous to that in Eq. (3.11).] The even Green's functions possess the same perturbative expansion as in the usual ϕ^4 theory except for a change of sign of the coupling constant, so again the sign of the beta function reverses:

$$\beta(g) = -27 \left(\frac{g}{2\pi} \right)^2. \quad (5.20)$$

This theory is asymptotically free. Furthermore, in the nonperturbative regime it exhibits parity symmetry breaking, but possesses \mathcal{PT} symmetry because G_1 is imaginary.

The other regime is even more interesting. If $m^2 < 0$ it is consistent to proceed in analogy with our treatment of the ϕ^3 theory above. We may assume a perturbative solution of the form $G_n \sim g^{n/2-1}$, as we have already seen in Eq. (3.13). Then we have a purely imaginary vacuum expectation value of the field, from Eq. (2.16):

$$G_1 = \sqrt{\frac{m^2}{g}}, \quad (5.21)$$

while the leading two-point function has the usual form of a propagator:

$$\tilde{G}_2(p) = \frac{1}{p^2 + M^2}. \quad (5.22)$$

Here the renormalized mass in leading order is positive:

$$M^2 = m^2 - 3gG_1^2 = -2m^2. \quad (5.23)$$

The leading three-point function has an evident diagrammatic interpretation:

$$\tilde{G}_3(p, q) = 6gG_1 \frac{1}{p^2 + M^2} \frac{1}{q^2 + M^2} \frac{1}{(p+q)^2 + M^2}. \quad (5.24)$$

The tree-level four-point function is easily extracted from Eq. (5.19):

$$\begin{aligned} \tilde{G}_4(p, q, r) &= \frac{6g}{(p^2 + M^2)(q^2 + M^2)(r^2 + M^2)[(p+q+r)^2 + M^2]} \\ &\times \left[1 + \frac{3m^2}{(p+q)^2 + M^2} + \frac{3m^2}{(p+r)^2 + M^2} + \frac{3m^2}{(q+r)^2 + M^2} \right], \end{aligned} \quad (5.25)$$

being composed of contributions from primitive four-point and three-point vertices.

Now we have perturbative parity symmetry breaking: the scalar field acquires a vacuum expectation value comparable to that of the gauge bosons in the standard model, $\sqrt{g}G_1$. Further, it appears likely that the theory is asymptotically free, because the sign of the four-point vertex is reversed. Indeed, apart from one-particle-reducible graphs, Eq. (5.25) gives just the usual primitive vertex in the high momentum limit, except for a change in sign. The theory is renormalizable because, apart from divergences associated with the 2-, 3-, and 4-point functions, no additional divergences occur. This is due to the fact that, for example, the 5-point function has no primitive vertices, as can be easily seen from the next in the sequence of Schwinger-Dyson equations after Eq. (5.18). The lowest order diagrams contributing to G_5 are as sketched in Fig. 5.

We have shown that the signs of the beta functions for a conventional $g\phi^3$ theory and for a \mathcal{PT} -symmetric $ig\phi^3$ theory in six space-time dimensions are reversed. Thus, while the former theory is asymptotically free, the latter is not. Similarly, the beta functions for a conventional $g\phi^4$ theory and for a \mathcal{PT} -symmetric $-g\phi^4$ theory in four space-time dimensions are reversed. Thus, while the former theory is not asymptotically free, the latter is. Similarly, as we have already argued in Ref. [12], we believe that while conventional quantum electrodynamics is not asymptotically free, \mathcal{PT} -symmetric electrodynamics is asymptotically free and possesses a nontrivial fixed point.

One of us, CMB, thanks Arthur Lue for many useful discussions at the Aspen Center for Physics. This work was supported in part by the U.S. Department of Energy.

REFERENCES

- [1] C. M. Bender and S. Boettcher, Phys. Rev. Lett. **80**, 5243 (1998).
- [2] C. M. Bender, S. Boettcher, and P. N. Meisinger, J. Math. Phys. **40**, 2201 (1999).
- [3] C. M. Bender and K. A. Milton, Phys. Rev. D **55**, R3255 (1997).
- [4] Field theoretic Hamiltonians that are both supersymmetric and \mathcal{PT} symmetric are examined in C. M. Bender and K. A. Milton, Phys. Rev. D **57**, 3595 (1998).
- [5] C. M. Bender, G. S. Guralnik, R. W. Keener, and K. Olaussen, Phys. Rev. D **14**, 2590 (1976).
- [6] C. M. Bender, F. Cooper, P. N. Meisinger, and V. M. Savage, submitted.
- [7] M. Abramowitz and I. A. Stegun, *Handbook of Mathematical Functions* (National Bureau of Standards, Washington, 1964), p. 831.
- [8] *Higher Transcendental Functions*, ed. by A. Erdélyi, (McGraw-Hill, New York, 1953), Vol. II, Chaps. 8 and 10.
- [9] G. Szegö, *Orthogonal Polynomials* (American Mathematical Society, New York, 1939), Chap. 6.
- [10] C. M. Bender, H. F. Jones, and V. M. Savage, submitted.
- [11] T. Muta, *Foundations of Quantum Chromodynamics* (World Scientific, Singapore, 1987), p. 217.
- [12] C. M. Bender and K. A. Milton, J. Phys. A: Math. Gen. **32**, L87 (1999).

FIGURES

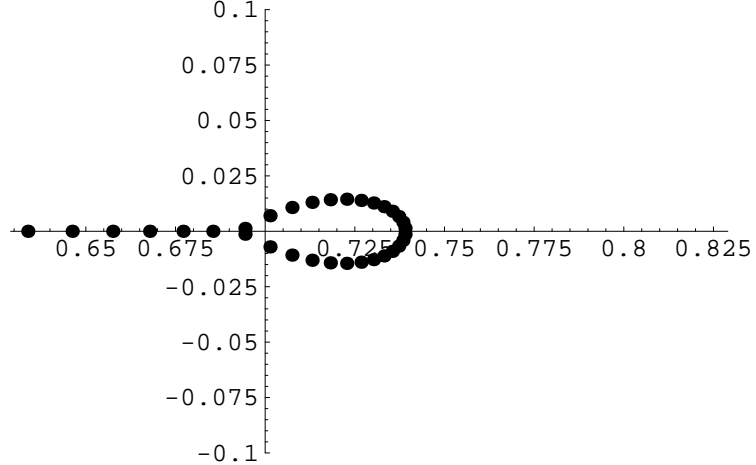


FIG. 1. Solutions of the first 150 coupled Schwinger-Dyson equations for the dimensionless one-point Green's function $iG_1g^{1/3}$ for the case of a massless zero-dimensional $N = 3$ theory. Note that the solutions (indicated by dots) lie in a small portion of the complex plane very close to the exact answer 0.72901.

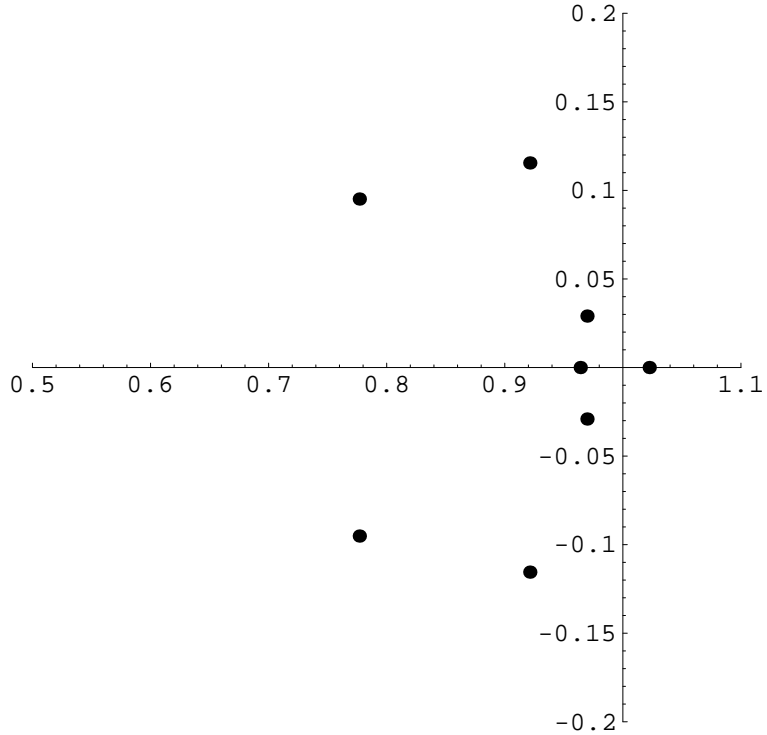


FIG. 2. Solutions of the first ten coupled Schwinger-Dyson equations for the dimensionless one-point Green's function $iG_1g^{1/4}$ for the case of a massless zero-dimensional $N = 4$ theory. The solutions (indicated by dots) lie in a small portion of the complex plane very close to the exact answer 0.97774.

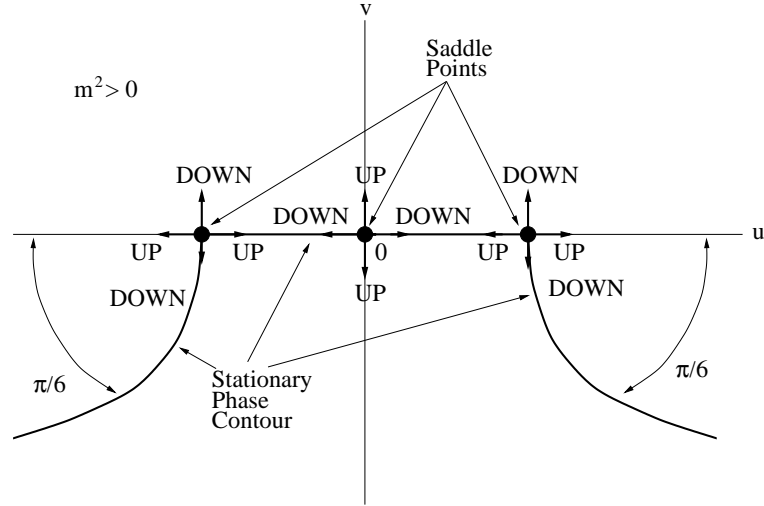


FIG. 3. Saddle points and steepest-descent paths for the function $\rho(x)$ in Eq. (3.9) for the case $m^2 > 0$.

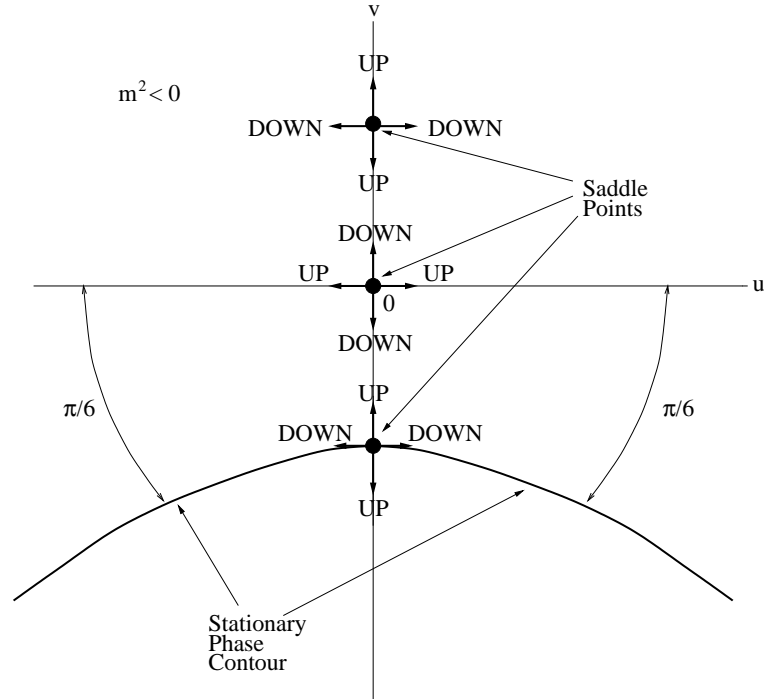


FIG. 4. Saddle points and steepest-descent paths for the function $\rho(x)$ in Eq. (3.9) for the case $m^2 < 0$.

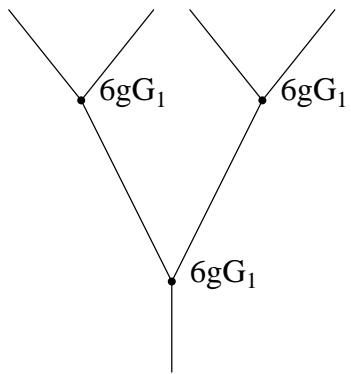
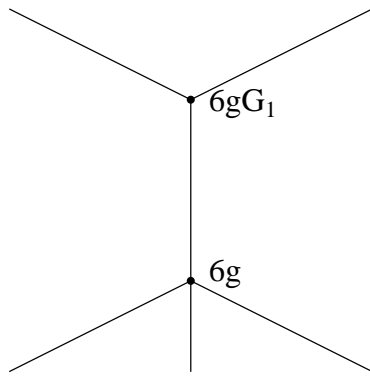


FIG. 5. Lowest order graphs contributing to G_5 .

TABLES

TABLE I. Exact values $iG_1^{\text{exact}} g^{1/N}$ and $G_2^{\text{exact}} g^{2/N}$ [see Eqs. (3.2) and (3.3)] compared with the first approximations $iG_1^{\text{SD}} g^{1/N}$ and $G_2^{\text{SD}} g^{2/N}$, which are obtained from the first two Schwinger-Dyson equations and given in Eqs. (3.5) and (3.6). This is done for the three cases $N = 3$, $N = 4$, and $N = 5$. Observe that the percent error increases with N for G_1 and decreases with N for G_2 . These trends continue until G_1 has a maximum error of 23.2% at $N = 53$, and until G_2 has a minimum error of 0.34% at $N = 8$. For $N > 53$ the error for G_1 decreases until it levels off at 21.3%. For $N > 8$ the error for G_2 increases like N . The large- N behavior of our approximations is more fully discussed later.

N	$iG_1^{\text{exact}} g^{1/N}$	$iG_1^{\text{SD}} g^{1/N}$	$G_2^{\text{exact}} g^{2/N}$	$G_2^{\text{SD}} g^{2/N}$
3	0.72901	0.79370	0.53146	0.27516
4	0.97774	1.10668	0.28000	0.14907
5	1.07865	1.24829	0.16433	0.10158

TABLE II. Exact values of iG_1^{exact} and $M^{\text{exact}} = E_1 - E_0$ (see Ref. [1]) compared with the first approximations iG_1^{SD} and M^{SD} , which are obtained from the first two Schwinger-Dyson equations (4.3) and (4.4). This is done for the three cases $N = 3$, $N = 4$, and $N = 5$. Note that the error is worse than for the zero-dimensional theories, and that the error for M increases with N . However, the error for iG_1 is smallest for $N = 4$.

N	iG_1^{exact}	iG_1^{SD}	M^{exact}	M^{SD}
3	0.59007	0.37011	2.95293	2.70192
4	0.86686	0.82548	4.52620	3.63424
5	1.01310	1.15416	6.70000	4.72160

TABLE III.

Schwinger-Dyson approximations for M_n compared with exact values of the energy difference, $E_n - E_0$, calculated in Ref. [1]. These approximations are based on the truncation of the first three Schwinger-Dyson equations for an $ig\phi^3$ field theory of the type in Eq. (1.4). Notice that M_1 is greater than the numerical result in this case, while in Table II, M_1 was less than the numerical answer. This suggests that in one dimension the oscillatory nature of successive approximations is present once again. Moreover, the percent error has decreased significantly; the error is 8.50% for M_1 calculated using the first two Schwinger-Dyson equations compared with 3.52% calculated using the first three Schwinger-Dyson equations.

n	$E_n - E_0$	M_n^{SD}	% error
1	2.952962	3.056763	3.52
2	6.406007	6.191828	3.34
3	10.158155	9.610135	5.39
4	14.135286	12.871434	8.94
5	18.295263	15.681836	14.28